

Instrumented pressure testing chamber for characterizing sediment cores recovered at in situ hydrostatic pressure

T.S. Yun ^{a,b}, G.A. Narsilio ^{a,b}, J.C. Santamarina ^{a,b,1}, C. Ruppel ^{a,c,*}

^a Georgia Institute of Technology, Atlanta, GA 30332, USA

^b School of Civil and Environmental Engineering, Georgia Tech, 790 Atlantic Drive NW, Atlanta, GA 30332-0355, USA

^c School of Earth and Atmospheric Sciences, Georgia Tech, Atlanta, GA 30332-0340, USA

Received 8 November 2005; received in revised form 22 March 2006; accepted 28 March 2006

Abstract

Marine sediments retrieved with pressure coring systems such as those used by the Integrated Ocean Drilling Program maintain samples at in situ hydrostatic pressure throughout recovery. Such pressure cores are particularly important for the study of gas hydrate-bearing sediments, which must be maintained within the gas hydrate stability field during shipboard core characterization. Until now, there has been no device capable of directly measuring a suite of physical properties on sediments contained in pressure cores without first depressurizing them. This study describes the design, construction, and deployment of the Instrumented Pressure Testing Chamber (IPTC), which was first used to measure the physical properties of pressure cores recovered ~1530 m below the sea surface during 2005 drilling in the Gulf of Mexico. The IPTC permits drilling through the plastic liner while the core is under pressure and the sequential measurement of P- and S-wave velocities, undrained strength, and electrical conductivity. Preliminary results indicate that the seismic velocities measured on a pressure core with the IPTC are more representative of in situ seismic velocities at comparable depths than are velocities measured on conventional cores from these same depths. The flexibility of the IPTC design allows future modifications to account for restoration of effective, not just hydrostatic, stress; the addition of new types of measurements; sampling of pore fluids and sediments under pressure; and use of the device as a laboratory reactor for gas hydrates studies.

© 2006 Elsevier B.V. All rights reserved.

Keywords: gas hydrate; pressure core; marine sediment; physical properties; Ocean Drilling Program; Gulf of Mexico

1. Introduction

The goals of sediment coring activities that rely on either traditional methods (gravity or piston coring) or

deep ocean drilling are to provide direct samples of material for a range of scientific studies and, in some cases, to recover samples that best represent in situ physical and chemical conditions. Even with piston coring technology, which arguably leaves sediment more intact than other types of coring, the recovery of sediment cores is accompanied by high strain, the loss of fluid pressure, and changes in temperature. For studies of the physical and geotechnical properties of cores, the best sampling techniques would create minimal sediment disturbance and maintain temperature, in situ pore fluid pressure, and effective stress during core recovery.

* Corresponding author. National Science Foundation, Division of Ocean Sciences, 4201 Wilson Blvd, Rm 725, Arlington, VA 22230, USA. Tel.: +1 703 292 7575.

E-mail addresses: taesup.yun@ce.gatech.edu (T.S. Yun), guillermo.narsilio@ce.gatech.edu (G.A. Narsilio), carlos@ce.gatech.edu (J.C. Santamarina), cdr@eas.gatech.edu (C. Ruppel).

¹ Tel.: +1 404 894 7605.

To meet some of the challenges associated with collecting samples that more closely represent in situ conditions, researchers have designed and deployed a number of so-called “pressure coring” systems capable of maintaining in situ pore fluid pressure during recovery of a sediment sample. Pressure coring technology includes the PCS (pressure core sampler), a small chamber that recovers samples that can then be depressurized for determination of gas quantities (e.g., Dickens et al., 1997, 2003; Milkov et al., 2004); Fugro and HYACE pressure corers, which recover approximately 1-m-long cores in plastic liners in unlithified and sublithified sediments, respectively (e.g., Leg 204 Shipboard Scientific Party, 2003); and the Pressure Temperature Core Sampler (PTCS) built for the Japan National Oil Corporation and capable of maintaining both pressure and temperature of recovered cores (Takahashi and Tsuji, 2005). Increasingly, scientists are conducting X-ray computed tomography scans and collecting multisensor track data on pressure cores while the cores are still under pressure (Leg 204 Shipboard Scientific Party, 2003).

Pressure coring has proved particularly important in the study of marine methane hydrate provinces. Gas hydrate, a naturally occurring crystalline compound composed of water and encapsulated low molecular weight gas, is stable over a limited pressure and temperature range. These unique pressure and temperature stability conditions challenge characterization and research efforts. During the recovery of standard cores, changes in temperature and especially pressure typically lead to the onset of gas hydrate dissociation. Pressure and temperature changes in boreholes during coring can also lead to perturbation of the gas hydrate stability field in situ, possibly affecting the quality and reliability of standard borehole logs in these settings.

This paper describes the first experiments ever undertaken to directly measure a suite of physical properties in sediments recovered by pressure coring devices and held at in situ fluid pressure. We describe the design of Georgia Tech’s Instrumented Pressure Testing Chamber (IPTC), which measures seismic velocities, undrained strength, and electrical conductivity of pressure cores, and discuss the first results obtained on

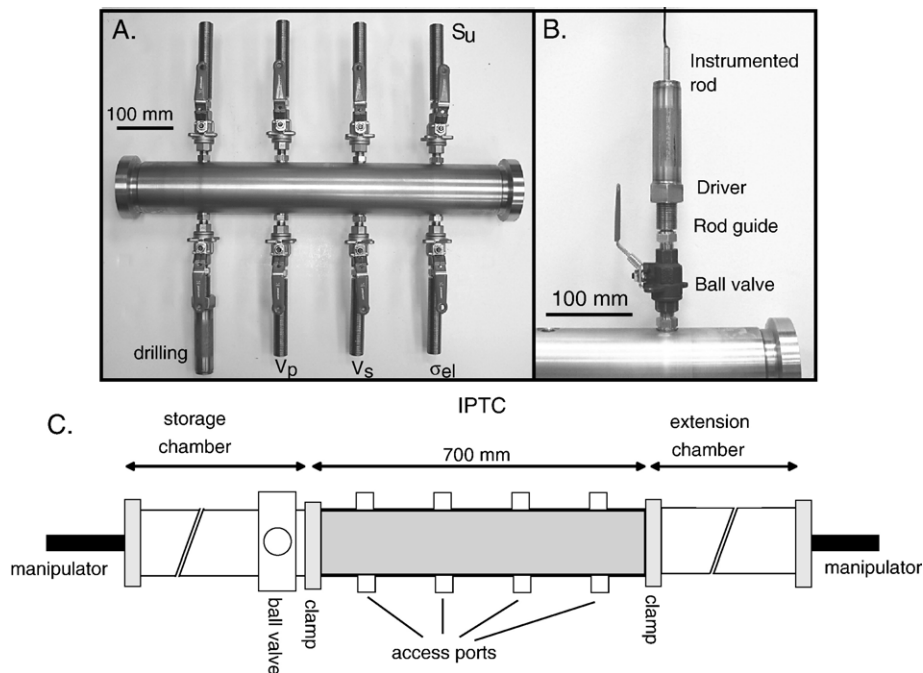


Fig. 1. (A) Photograph of IPTC, which consists of a stainless steel vessel with 4 two-sided instrumentation ports. The purpose of each port is as indicated, with drilling occurring in the ports closest to the point at which the pressure core is inserted into the IPTC. Note that undrained shear strength S_u and electrical conductivity σ_{el} are measured at the same lateral position in the core but through different sides of the paired access ports. (B) Each port shown in (A) has an instrumented rod, driver, rod guide and ball valve. The interior of the IPTC, which is kept at in situ hydrostatic pressure, is accessible through the ball valve at the base of the assembly. (C) Schematic of the complete system used to transfer the pressure core to the IPTC and to manipulate the core once inside the chamber. The IPTC is connected to the storage chamber on the left and the extension chamber on the right through ball valves. The longitudinal movement of the pressure core is controlled by manipulators. The storage chamber, extension chamber, and manipulators were provided by Geotek, Ltd.

sediment cores recovered in a Gulf of Mexico gas hydrate province.

2. IPTC development and use

2.1. IPTC design

The IPTC consists of a 316 stainless steel pressure chamber (Fig. 1) with ports to provide access to the sediment core. The IPTC's wall thickness ($t=12.5$ mm) can sustain a fluid pressure of ~ 36 MPa even in the presence of the access ports. The inside diameter ($d_{in}=65$ mm) of the IPTC accommodates pressure cores recovered by the Fugro pressure coring system (63-mm-diameter), and an auxiliary tube fits inside the IPTC for analysis of smaller (57-mm-diameter) HYACE rotary (pressure) cores. The IPTC is designed to ensure workability, safety (Environment, Safety, and Health Manual, 2003), and geometric compatibility with peripheral devices and instrumentation.

To gain access to the sediment core for physical properties measurements, the IPTC pressure chamber has two parallel rows of 4 instrumentation arms (Fig. 1A), each consisting of a stainless steel rod ($L=300$ mm, $d=8$ mm), a driver, a rod guide, and a ball valve (Fig. 1B). Three of the instrumented rod pairs contain transducers (Fig. 2) that are introduced into the sediments using the mechanical advancing driver through holes previously made with a drilling rod, which occupies the first access port closest to the point at which the core is introduced into the IPTC. Instrumented rods penetrate into the pressurized chamber through 25.4-mm-diameter rod guides. The inside hole houses a high-pressure O-ring, which can accommodate the rotation, oscillation, and helicoidal motion of instrumented rods while withstand-

ing ~ 30 MPa. A ball valve lies between the rod guide and the chamber to permit tool replacement or repair while the system is under pressure. The O-rings are rated for -45 to 200 °C, which we consider to be the full theoretical operating range of the IPTC. Thus, the IPTC could be operated at temperatures well below 0 °C.

The rod guides are externally threaded. The matching threaded driver advances along the externally threaded rod guide, thereby pushing the instrumented rods. The longitudinal force on a rod is ~ 1 kN under 20 MPa chamber pressure, and 7.6 Nm of torque is required to rotate the driver. Flat ball bearings between the instrumented rods and drivers minimize friction, facilitate drilling of holes, and prevent the rotation of direction-dependent transducers. The length of the rod guide is designed to allow complete retrieval of instrumented rods so the ball valve can be closed, preserving the pressure in the chamber.

2.2. Transfer of pressure cores into the IPTC

As noted above, the IPTC uses pressure cores obtained with third-party technology. It is thus necessary to transfer the pressure core into the IPTC without releasing pressure on the sample. The transfer system, which consists of manipulators, a storage chamber, and an extension chamber manufactured and operated by Geotek, Ltd., is shown in relation to the IPTC in Fig. 1C.

To transfer the pressure core from its storage chamber into the IPTC, the IPTC is quick-clamped on one end to a ball valve system on the storage chamber and on the other end to an extension chamber that permits introduction of a manipulator to handle the core's movement through the IPTC. Once the inside pressure of the IPTC and the extension chamber are equalized with the fluid pressure in the storage chamber, the ball valve in the storage chamber can be opened. Using position manipulators at both ends of the system, the pressure core is first grabbed and then controlled from both ends as it slides into the IPTC without rotation.

3. Measurements and methods

Conducting IPTC measurements on a recovered sediment core requires first drilling two diametrically opposed holes through the plastic liner while the specimen is under pressure. To identify optimal drill bit characteristics, we tested various commercially available drill bit designs with the plastic liner at low temperature. The best performing drill bit had a pilot tip, flute bit, no wing bit, and a large-angle cone shaped tip.

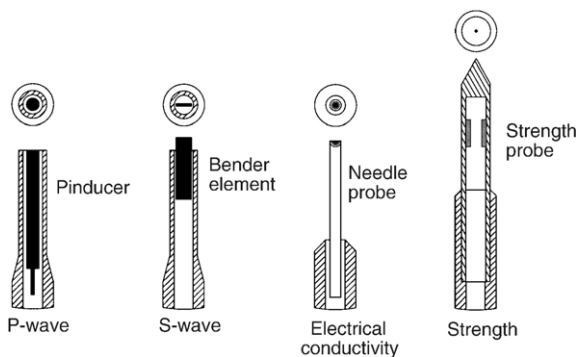


Fig. 2. Diagrams of the sensors embedded at the end of the 300-mm-long instrumented rods. Electrical wiring for the sensors comes out through the other end of the rod, and the void space in the rod is filled with epoxy to maintain fluid pressure.

The selected drill bit is mounted at the end of an 8-mm-diameter and 300-mm-long stainless steel rod.

Fig. 3 shows the configuration of peripheral electronics and other components of the data acquisition system. The digital oscilloscope captures the signals for P- and S- wave measurements as well as the voltage output for the electrical conductivity. The computer logs the output from the multimeter at 1 s intervals. A multiple BNC adapter board facilitates switching connections between different measurements to minimize duplicating electronics and to simplify the measurement procedure.

3.1. Seismic velocities

P-wave and S-wave velocities, electrical conductivity, and undrained shear strength of the sediment core are sequentially measured through the 3 instrumentation ports arrayed along the IPTC beyond the drilling port. For the P- and S-wave measurements, rod endings are trimmed into 6 mm outside diameter tips to facilitate introduction of transducers into drilled holes. P-wave measurements are conducted with miniature pinducer barrels and connecting coaxial cables that are placed inside respective rods and that are fixed with a high strength epoxy. The impulse generator provides the input signal, and received signals are filtered and amplified, before being digitized at 1 MHz and stored. For both the P- and S-wave measurements, noise control is based on signal stacking (typically 1024 signals). To determine velocities, we pick first arrivals from stacked waveforms.

Bender elements are used for S-wave measurements. The bender elements, which are 10 mm long and 4 mm wide, stick out at the end of rods to attain optimal transducer-sediment coupling for signal generation and detection. Bender elements and connecting co-axial

cables are fixed to the rod with epoxy. The signal generator produces input square waves, and output signals are filtered and amplified, then digitized at 400 kHz and stored.

3.2. Electrical conductivity

Electrical conductivity is measured using the single-wedge electrical needle probe (Cho et al., 2004) that sticks out 2.5 cm ahead of the rod. The optimal operating frequency to prevent resonance and electrode effects is 100 kHz, which was selected by conducting spectral measurements with a low frequency impedance analyzer. To measure conductivity, which is the inverse of resistivity, the needle probe is connected in series to a known resistor ($R_{\text{known}}=100 \Omega$). The resistance at the needle tip R_{needle} is computed from:

$$R_{\text{needle}} = \frac{V_{\text{out}}}{V_{\text{in}} - V_{\text{out}}} \cdot R_{\text{known}}, \tag{1}$$

where V_{out} is the voltage drop across the needle and V_{in} is the voltage at the resistor tip. V_{in} and V_{out} are captured by a digital oscilloscope. The measured resistance R_{needle} is related to the sediment conductivity σ_{el} through the shape factor β according to $\sigma_{\text{el}} = \beta \cdot (R_{\text{needle}})^{-1}$. The shape factor $\beta=373 \text{ m}^{-1}$ is experimentally determined using electrolytes of known conductivity.

3.3. Strength

Strength is measured using a specially designed, 60° cone-shaped stud. A full-bridge strain gauge circuit is mounted on the inner wall of the cone tube so that the cone effectively acts as a load cell. The cone is fixed to the rod with epoxy. The bridge is fed a DC voltage, and the cross bridge potential is automatically logged at 1 s intervals. The load cell cone tip is calibrated by gravity loading to relate the applied force F to the measured voltage output V_{out} as $F = \alpha \cdot V_{\text{out}}$, where α is a calibration factor of 134.3 N/mV. The cone resistance q_c is related to the measured force F through the cone area $A_c = 0.246 \text{ cm}^2$. Finally, the cone resistance q_c is a function of the unknown sediment undrained shear strength S_u .

Various theories relate S_u to q_c , including bearing capacity type analyses (Terzaghi, 1943; Meyerhof, 1951), cavity expansion theories (Vésic, 1972, 1977), strain path methods (Baligh, 1985; Houlsby and Teh, 1988), and semiempirical methods (Konrad and Law, 1987). In its simplest form, $S_u = q_c / N$. Empirical observations indicate that N can vary between 4 and 30 depending on factors such as lateral stress, soil plasticity,

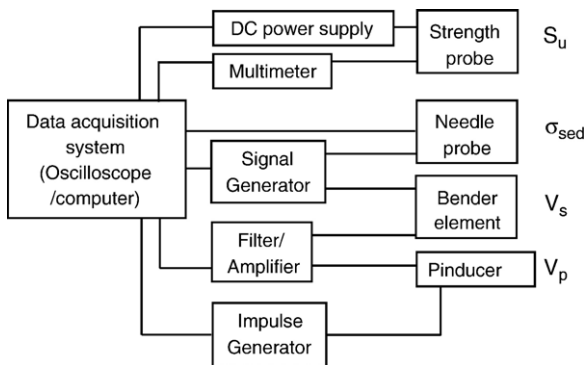


Fig. 3. Schematic diagram of data acquisition system and electronics for the IPTC.

stress history, and stiffness (Terzaghi, 1943; Meyerhof, 1951; Kurup and Tumay, 1998; Koumoto and Houlby, 2001; Mesri, 2001). N is often assumed to be 10 to 15 for soft sediments. Finally, the undrained shear strength is determined from the measured output voltage V_{out} as:

$$S_u = \frac{q_c}{N} = \frac{F}{A \cdot N} = \frac{\alpha \cdot V_{\text{out}}}{A \cdot N} \quad (2)$$

3.4. Calibration and testing

The IPTC was tested and the velocity sensors calibrated by conducting experiments on 3 samples: compacted Georgia silt, saturated sand, and frozen sand. The first 2 samples were tested to 17 MPa fluid pressure, while the frozen sand was tested up to 1 MPa. In each case, the samples were pressurized with water during the measurement of the seismic velocities. The results of the experiments demonstrated that the P- and S-wave sensors functioned properly under high pressures and that the sensors were properly coupled to the samples, which is a particular concern with the frozen sand that is most analogous to gas hydrate. The electrical conductivity and strength sensors were calibrated as detailed in Sections 3.2 and 3.3, respectively.

4. Results

4.1. Field test

The IPTC was deployed for the first time during spring 2005 drilling in the Gulf of Mexico as part of the ChevronTexaco Joint Industry Project on Methane Hydrates. We here report data from Keathley Canyon lease block 151 (Fig. 4). The focus area for the KC151 drilling lies in ~ 1322 m of water on a structural ridge that forms the edge of a salt withdrawal mini-basin. A regional bottom simulating reflector (BSR) attests to the presence of gas hydrate at ~ 415 m below seafloor (mbsf) at the drilling site (Hutchinson et al., 2005).

During the drilling expedition, we were given access to a Fugro pressure core that was recovered at 227 m below seafloor (mbsf) in hole KC151-3 (26.823°N , 92.9867°W). The pressure core was successfully transferred into the IPTC ~ 20 h after recovery, under fluid pressure maintained at ~ 14 MPa, slightly lower than the nominal in situ hydrostatic pressure of 15.6 MPa. From standard laboratory analyses we conducted on conventional cores collected at approximately the same depth, we classify the high specific surface ($> 62 \text{ m}^2/\text{g}$) clayey sediment as CH (inorganic clay of high plasticity) in the Unified Soil Classification System.

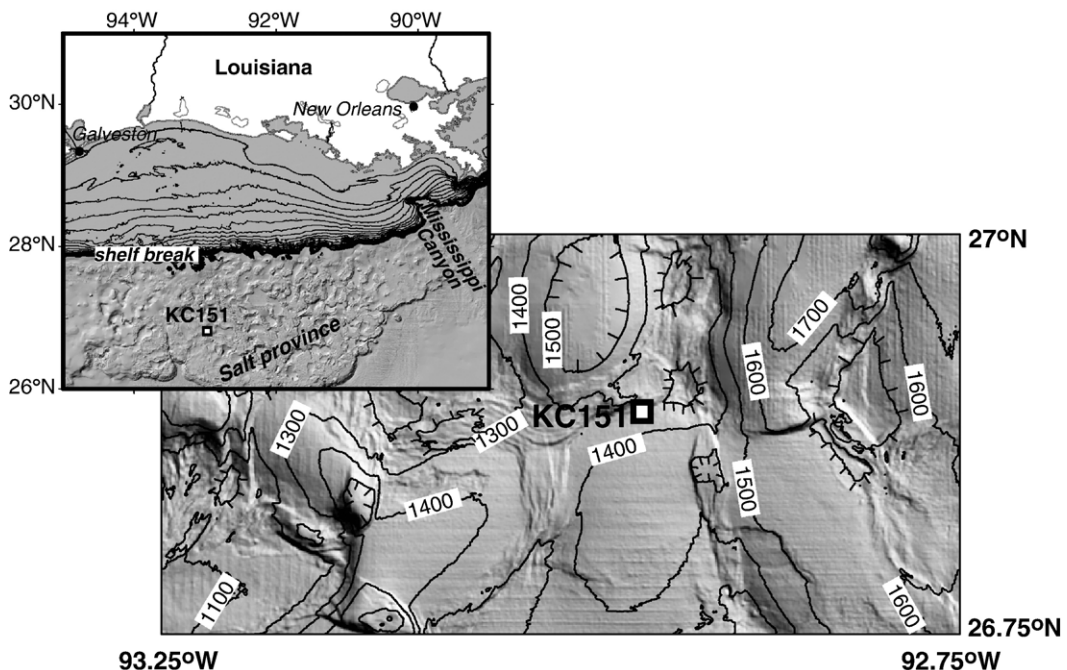


Fig. 4. The location of 2005 drilling led by the ChevronTexaco Joint Industry Project on Methane Hydrates at ~ 1300 m water depth in the Gulf of Mexico is shown by the square. The pressure core used in this study was recovered from 227 mbsf in Keathley Canyon lease block 151 (KC151) along a ridge between salt withdrawal mini-basins. Contour interval is 100 m. Shaded relief map provided by the USGS Coastal Marine Geology Program (D. Hutchinson, pers. comm., 2003). Inset shows the location of Keathley Canyon relative to key features of the northern Gulf of Mexico.

Although there was clear evidence for gas in all of the conventional cores recovered at depths bracketing the pressure core, gas hydrate was neither identified visually nor detected indirectly with other analyses. In addition, although the pressure core was maintained at ~ 14 MPa fluid pressure throughout the recovery and analysis period, the ambient air temperature in the laboratory van in which the IPTC was operated was ~ 7 to 8 °C or lower. To ensure that the sediment core remained within the stability field for gas hydrate in case any were present, ice was packed around the IPTC.

4.2. Physical properties measurements

We first performed noninvasive P-wave scanning of the core through the plastic liner, collecting data every 3 cm. Holes were then drilled at discrete locations in the liner, and the core was advanced to line up the drillholes with the seismic transducers. As the core was moved through the IPTC, we pushed the instrumented rods into the sediment through the drilled holes and recorded P- and S-wave data at successive locations on the core. Fig. 5 depicts the invasive P- and S-wave velocity data and the

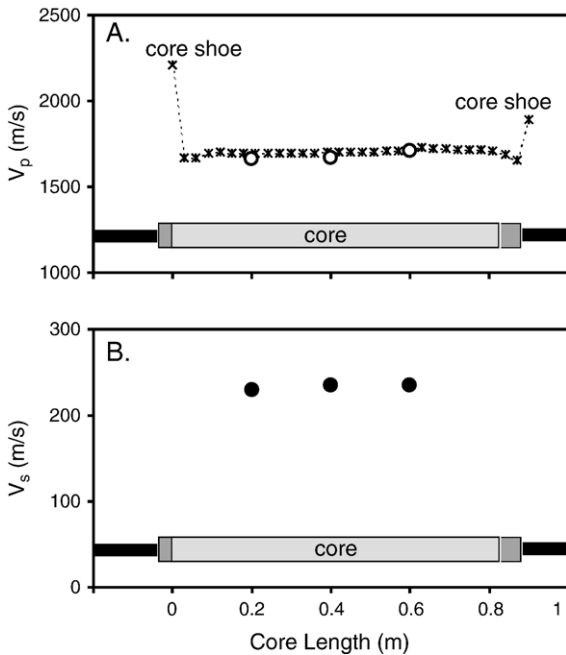


Fig. 5. Elastic wave velocities measured with the IPTC. (A) Noninvasive P-wave velocities measured continuously through the core liner with the IPTC are shown by dotted curve. Velocities measured at discrete locations in the specimen through invasive measurements with the P-wave transducers introduced into holes drilled through the liner are indicated by the open circles. (B) Invasive S-wave measurements at discrete locations in the pressure core.

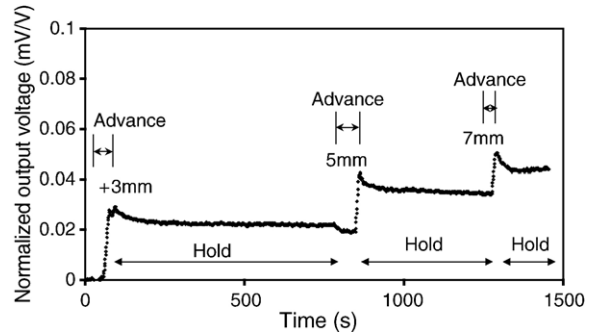


Fig. 6. Voltage evolution with time at different penetration depths in the IPTC core specimen during the measurement of S_u .

noninvasive P-wave velocity profile from the IPTC measurements. For the invasive data, the measured P-wave velocities are 1601 to 1629 m/s, and the S-wave velocities range from 229 to 235 m/s. Noninvasive P-wave velocities at the locations of the drilled holes vary from 1653 to 1729 m/s.

Strength was determined using liner perforations on one side of the specimen. As the cone tip penetrated the specimen, the penetration resistance was monitored. As shown in Fig. 6, the peak voltage output attained during penetration is followed by the asymptotic decay during holding periods. Using (2) and $N=10$ and 15, we estimate the undrained shear strength to be between $S_u=245$ and 330 kPa. Fig. 6 also shows that the penetration resistance increases with penetration depth in the sample. This may reflect varying degrees of sample disturbance near the plastic liner, enhanced confinement away from the liner, or the contribution of cone shaft friction. We cannot assess these factors with this preliminary data set.

Electrical conductivity was measured at the same core location as the strength measurement, but using the drillhole on the opposite side of the core. Measured values are $\sigma_{el}=3.3\pm 0.3$ S/m. Although the methodology has been extensively tested and applied (Cho et al., 2004), we consider the value measured on this pressure core unreliable due to a variety of factors (e.g., incomplete penetration of the core by the sensor).

5. Discussion

5.1. Comparison of pressure cores and conventional cores

The physical properties of sediments recovered through coring are typically measured on cores held at atmospheric pressure. To the best of our knowledge, the initial deployment of the IPTC represents the first time that a suite of physical properties has been measured

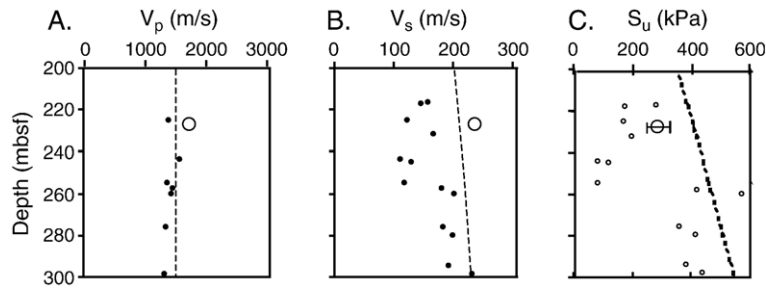


Fig. 7. Comparison between conventional core data (solid dots) and pressure core results (open circle) gathered at the KC 151-3 site. The panels show results for conventional cores and the pressure core between 200 and 300 mbsf. (A) P-wave velocity V_p . The dashed line indicates seawater V_p of 1480 m/s. (B) S-wave velocity V_s . The dashed line represents the empirical relationship $V_s = 22.5[\sigma'_m / (1 \text{ kPa})]^{0.3}$ after *Stokoe et al. (1991)*, where σ'_m is the effective mean stress in the polarization plane. (C) Undrained shear strength S_u . The dashed line shows the empirical relationship $S_u = 0.22 \sigma'_v$, where σ'_v denotes vertical effective stress, after *Mesri (1989)*.

invasively on sediment cores maintained at in situ fluid pressure since recovery. To evaluate the importance of undertaking physical properties measurements at in situ fluid pressure, we compare preliminary IPTC results to data obtained from conventional cores recovered at comparable depths.

Fig. 7 summarizes the comparison between IPTC measurements and measurements on conventional cores. Compared to conventional cores at the same depths, the IPTC cores have compressional and shear wave velocities that are 22% and 64% higher, respectively. We can also compare the IPTC results to those obtained in situ through logging while drilling (LWD). LWD yielded average V_p and V_s of 1720 and 300 m/s, respectively, for the 10 readings closest to the nominal depth of the pressure core. Compared to the IPTC data,

the LWD results are 2% higher for V_p and 29% higher for V_s (Fig. 8). Based on these preliminary findings, the IPTC measurements appear to be more representative of in situ (LWD) values than are measurements conducted on conventional cores.

The value of V_p is strongly affected by confining pressure when gas comes out of solution in otherwise saturated soft sediments. The disparity among V_s values measured using the 3 approaches (i.e., conventional cores, pressure cores in the IPTC, and LWD; Fig. 8) is greater than that among V_p values because V_s depends on shear modulus, which in turn depends on the skeletal stiffness of samples. Skeletal stiffness is strongly affected by coring procedures and effective stress release, particularly in diagenetically cemented sediments.

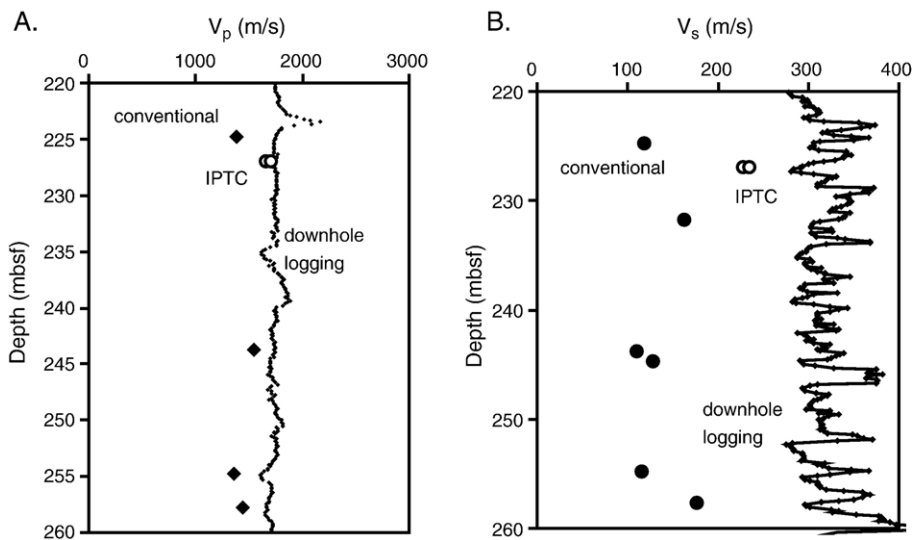


Fig. 8. Comparison between conventional core data (solid dots), downhole logging data (continuous curve) and IPTC measurements (open circles) for (A) P-wave velocity and (B) S-wave velocity in the depth range that brackets the sample tested in the IPTC.

Compared to conventional cores taken just above and below the pressure core, the IPTC core has undrained shear strength 1.7 times as large (Fig. 7C). The specimen's undrained shear strength is dominated by the effective stress history and the ability to generate pore pressure during shear. Once again, fabric disturbance and gas dissolution result in low S_u values in conventional coring operation and render pressure coring and testing with the IPTC the preferred methodology for measuring S_u .

5.2. Stress state

Although the effective stress is not controlled in the present IPTC prototype, it is partially “locked in” by wall friction between the sediment and the plastic core liner. In addition, maintaining high fluid pressure prevents or minimizes gas dissociation/expansion and the ensuing destruction of the sediment's microstructure (e.g., Francisca et al., 2005). Diagenetic cementation or high hydrate concentration (probably $S_{\text{hyd}} > 50\%$) may also help the soil fabric retain some of its structure during coring and recovery. Nonetheless, future generations of the IPTC will be designed to restore effective stress on the sample following transfer from the pressure coring chamber.

6. Conclusions

In this paper, we have described the design and construction of the IPTC, a new tool for the measurement of physical properties on pressure cores recovered and maintained at in situ hydrostatic pressure. Based on our P-wave scanning results, we conclude that this first deployment probably did not test a core that contained gas hydrate. Nonetheless, our results clearly indicate that seismic velocities and the undrained shear strength measured on the IPTC core are more representative of in situ seismic velocities than are those measured in the laboratory on conventional cores.

The IPTC design is very flexible and can be readily extended to accommodate more measurements, a different suite of measurements, or even experiments that require single or repeated access to the specimen. For example, the addition of more access ports and transducers would permit us to construct electrical resistivity tomographic images of cores. Alternately, the IPTC could be used to measure thermal or hydraulic parameters (e.g., thermal conductivity, hydraulic conductivity), to monitor pressure, temperature, and geochemical changes in the specimen (e.g., during the dissociation of gas hydrate), to sample sediments or pore fluids, or to conduct microbiological investigations.

As mentioned above, the best sampling and measurement device for samples containing gas hydrate would maintain temperature, pressure, and effective stress throughout testing. Currently, the IPTC can maintain in situ fluid pressure, but temperature is controlled by the ambient temperature of the testing laboratory or by operating the IPTC in an ice bath. In recent months, we have begun to operate the IPTC under controlled ambient temperature conditions in a portable freezer, an adaptation that greatly increases the potential uses of the device. In the immediate future, we are modifying the IPTC to restore effective stress on natural samples. Eventually, the IPTC should be applied not only to natural samples, but also to simulate the effects of coring (e.g., partial destabilization of gas hydrate in the laboratory) and to serve as a reactor for studying various physical, chemical, and/or biological phenomena in hydrate-bearing sediments.

Acknowledgements

We thank the crew of the *MSV Uncle John* for their work to obtain the cores, P. Schultheiss and J. Roberts of Geotek, Ltd. for use of the transfer and storage vessels and manipulators, and L. Stern for comments that improved the manuscript. This research was primarily supported by a contract to C.R. and J.C.S. from the Joint Industry Project for Methane Hydrate, administered by ChevronTexaco with funding from award DE-FC26-01NT41330 from DOE's National Energy Technology Laboratory. J.C.S. thanks the Goizueta Foundation at Georgia Tech for providing support for some aspects of this work. The research was completed while C.R. was on assignment at and wholly supported by the National Science Foundation (NSF). All findings are those of the authors and do not reflect the views of the DOE or NSF.

References

- Baligh, M.M., 1985. Strain path method. *J. Geotech. Eng.* 111, 1108–1136.
- Cho, G.C., Lee, J.-S., Santamarina, J.C., 2004. Spatial variability in soils: high resolution assessment with electrical needle probe. *J. Geotech. Geoenviron. Eng.* 130, 843–850.
- Dickens, G.R., Paull, C.K., Wallace, P., ODP Leg 164 Scientific Party, 1997. Direct measurement of in situ methane quantities in a large gas hydrate reservoir. *Nature* 385, 426–428.
- Dickens, G.R., Schroeder, D., Hinrichs, K.-U., Leg 201 Scientific Party, 2003. The pressure core sampler (PCS) on ODP Leg 201: general operations and gas release. In: D'Hondt, S.L., Jørgensen, B.B., Miller, D.J., et al. (Eds.), *Proc. ODP, Init. Repts.*, vol. 201. College Station, Texas, pp. 1–22.
- Environment, Safety, and Health Manual, 2003. Document 18.2: pressure vessel and system design, Lawrence Livermore National Laboratory, online at: http://www.llnl.gov/es_and_h/hsm/doc_18.02/doc18-02.html.

- Francisca, F., Yun, T.S., Ruppel, C., Santamarina, J.C., 2005. Geophysical and geotechnical properties of near-surface sediments in the Northern Gulf of Mexico gas hydrate province. *Earth Planet. Sci. Lett.* 237, 924–939. doi:10.1016/j.epsl.2005.06.050.
- Houlsby, G.T., Teh, C.I., 1988. Analysis of the piezocone in clay. In: de Ruiter, J. (Ed.), *Penetration Testing*, Proc. First International Symp. Penetration Testing, Orlando, Florida, vol. 2, pp. 777–783.
- Hutchinson, D., Snyder, F., Hart, P.E., Ruppel, C.D., Pohlman, J., Wood, W.T., Coffin, R.B., Edwards, K.M., 2005. Geologic and site survey setting for JIP Gulf of Mexico gas hydrate drilling. *EOS Trans. Amer. Geophys. Union* 86 (Abstract OS43A-0618).
- Konrad, J.M., Law, K.T., 1987. Undrained shear strength from piezocone tests. *Can. Geotech. J.* 24, 392–405.
- Koumoto, T., Houlsby, G.T., 2001. Theory and practice of the fall cone test. *Geotechnique* 51, 701–712.
- Kurup, P.U., Tumay, M.T., 1998. Calibration of a miniature cone penetrometer for highway applications. *Transp. Res. Rec.* 1614, 8–13.
- Leg 204 Shipboard Scientific Party, 2003. Explanatory notes. In: Tréhu, A.M., Bohrmann, G., Rack, F.R., Torres, M.E., et al. (Eds.), *Proc. ODP, Init. Repts.*, 204, College Station, TX, pp. 1–102. Available from World Wide Web: http://www-odp.tamu.edu/publications/204_IR/VOLUME/CHAPTERS/IR204_02.PDF.
- Mesri, G., 1989. Re-evaluation of $S_u = 0.22\sigma'_p$ using laboratory shear tests. *Can. Geotech. J.* 26, 162–164.
- Mesri, G., 2001. Undrained shear strength of soft clays from push cone penetration test. *Geotechnique* 51, 167–168.
- Meyerhof, G.G., 1951. Ultimate bearing capacity of foundations. *Geotechnique* 2, 301–332.
- Milkov, A.V., Dickens, G.R., Claypool, G.E., Lee, Y.-J., Borowski, W.S., Torres, M.E., Xu, W., Tomaru, H., Trehu, A.M., Schultheiss, P., 2004. Co-existence of gas hydrate, free gas, and brine within the regional gas hydrate stability zone at the southern summit of Hydrate Ridge (Oregon margin): evidence from prolonged degassing of a pressurized core. *Earth Planet. Sci. Lett.* 222, 829–843.
- Stokoe, K.H., Lee, J.N.-K., Lee, S.H.-H., 1991. Characterization of soil in calibration chambers with seismic waves. In: Huang, A.B. (Ed.), *Proc. Symp. Calibration Chamber Testing*. Elsevier, Postdam, NY, pp. 363–376.
- Takahashi, H., Tsuji, Y., 2005. Multi-well exploration program in 2004 for natural hydrate in the Nankai-Trough offshore Japan. *Proc. Offshore Technology Conference*, OTC 17162.
- Terzaghi, K., 1943. *Theoretical Soil Mechanics*. John Wiley and Sons, New York, N.Y. 510 pp.
- Vésic, A.C., 1972. Expansion of cavities in infinite soil mass. *ASCE J. Soil Mech. Found. Div.* 98, 265–290.
- Vésic, A.S., 1977. *Design of Pile Foundations*, Synthesis of Highway Practice No. 42, Nat. Coop. Highway Research Prog. Transportation Research Board, Washington, D.C. 68 pp.